

The Tendency of FMR of a Patterned Synthetic Antiferromagnet

Yo Chan Kong*, Sangho Lim and Kyung-Jin Lee

Department of Materials Science and Engineering, Korea University, Seoul 136-713, Korea

1. Introduction

A synthetic antiferromagnet (SAF) is a tri-layer structure composed of two ferromagnets (FMs) separated by a normal metal (NM, typically thin Ru layer). The two FMs are exchange coupled across the NM whose thickness is adjusted to produce an antiferromagnetic coupling due to the Ruderman-Kittel-Kasuya-Yoshida (RKKY) interaction. The SAF is also used as a free layer structure in toggle-mode magnetic random access memory (MRAM) [1] and spin-transfer torque (STT) MRAM [2, 3]. In comparison to a single FM, the SAF as a free layer has advantages for the STT MRAM [2, 3]; the enhanced thermal stability of stored magnetic information due to the increased magnetic volume, and the reduced switching current density possibly due to the reduced effective magnetization.

In order to investigate the possibility of SAF as high frequency microwave devices, it is important to theoretically study the base FMR frequency at no external bias for a given SAF structure. An analytical solution of the FMR frequency in *unpatterned* SAF structures has been already proposed [10-12]. However, there is no report on the analytical solution of the FMR frequency in SAF structures patterned into submicrometer scale where the magnetostatic dipolar coupling between two FMs cannot be ignored in determining the FMR frequency. In this work, we derive the analytical equation of the FMR frequency in patterned SAF structure when $I = 0$ and $H < H_{SF}$ (spin-flop field). The theoretical result is verified by comparing to the macrospin model. Since the patterned SAF is used in most applications, our result can provide an important guideline to design and to interpret experiments utilizing the SAF structure.

2. Theory and Model

Fig. 1(a) shows the schematic of the patterned SAF structure. Here we focus on the case where the external field is smaller than the spin-flop field above which the magnetizations of two FMs are deviated from the perfectly antiparallel alignment. The equation of motion of magnetization \vec{M}_i is described by the Landau-Lifshitz-Gilbert (LLG) equation;

$$\frac{\partial \vec{M}_i}{\partial t} = -\gamma \vec{M}_i \times \vec{H}_i + \frac{\alpha}{M_i} \vec{M}_i \times \frac{\partial \vec{M}_i}{\partial t}, \quad (1)$$

Total fields acting on the free layer 1 (FM1) and the free layer 2 (FM2) are given by

$$\begin{aligned} \vec{H}_1 &= (H_1^{k_0} M_1^x / M_1 - \lambda_1^x M_2^x - N_1^x M_1^x, -\lambda_1^y M_2^y - N_1^y M_1^y, -\lambda_1^z M_2^z - H_{ext} - N_1^z M_1^z), \\ \vec{H}_2 &= (H_2^{k_0} M_2^x / M_2 - \lambda_2^x M_1^x - N_2^x M_2^x, -\lambda_2^y M_1^y - N_2^y M_2^y, -\lambda_2^z M_1^z - H_{ext} - N_2^z M_2^z), \end{aligned} \quad (2)$$

where $H_i^{k_0}$ is the crystalline anisotropy field of the FM_i, $M_1^z = +M_1$, $M_2^z = -M_2$, and M_1 (M_2) is the saturation magnetization of FM₁ (FM₂) ($|M_1^x|, |M_1^y| \ll M_1, |M_2^x|, |M_2^y| \ll M_2$). The coefficients λ and N are given by

$$\begin{aligned} \lambda_1^x &= -\lambda_1^{RKKY} + N_{21}^x, & \lambda_1^y &= -\lambda_1^{RKKY} + N_{21}^y, & \lambda_1^z &= -\lambda_1^{RKKY} + N_{21}^z \\ \lambda_2^x &= -\lambda_2^{RKKY} + N_{12}^x, & \lambda_2^y &= -\lambda_2^{RKKY} + N_{12}^y, & \lambda_2^z &= -\lambda_2^{RKKY} + N_{12}^z \end{aligned} \quad (3)$$

where $\lambda_i^{RKKY} = J_{ex}/(M_i^2 d_i)$, J_{ex} is the RKKY exchange energy through the Ru layer, d_i is the thickness of FM_i, N_{ij}^k is the k -component of the demagnetization factor corresponding to the magnetostatic field on the target FM_j originating from the source FM_i where $k = x, y$, and z , $N_{ii}^k = N_{ii}^k$, and H_{ext} is the external field applied along the $-z$ -axis. $N_i^x + N_i^y + N_i^z = 4\pi$ in the c.g.s. unit. The N_{ij}^k varies with varying geometric variables (L, W, t_{F1}, t_{F2} , and t_S) of the sample and its formula can be found in the ref. [13].

The magnetization motion in the thin-film geometry is elliptical precession around the z -axis with $M_{iy} = A \cos(\omega t)$, $M_{ix} = -B \sin(\omega t)$.

Then, one finds the FMR frequency f_{\pm} ,

$$f_{\pm} = \frac{\omega_{\pm}}{2\pi} = \frac{\gamma}{2\pi} \left(\frac{-b \pm \sqrt{b^2 - 4c}}{2} \right)^{1/2} \quad (4)$$

where

$$\begin{aligned} b &= -[\lambda_2^z M_1 + H + H_2^d](\lambda_2^z M_1 + H + H_2^k) + \lambda_1^y \lambda_2^x M_1 M_2 \\ &\quad - [\lambda_1^z M_2 - H + H_1^d](\lambda_1^z M_2 - H + H_1^k) + \lambda_1^x \lambda_2^y M_1 M_2 \\ c &= [\lambda_1^z M_2 - H + H_1^d](\lambda_1^z M_2 - H + H_1^k)[\lambda_2^z M_1 + H + H_2^d](\lambda_2^z M_1 + H + H_2^k) \\ &\quad - [\lambda_1^x \lambda_2^y M_1 M_2 - H + H_1^d][\lambda_2^z M_1 + H + H_2^d]\lambda_1^y \lambda_2^x M_1 M_2 \\ &\quad - \lambda_1^z \lambda_2^z M_1 M_2 (\lambda_1^z M_2 - H + H_1^k)(\lambda_2^z M_1 + H + H_2^k) + \lambda_1^x \lambda_1^y \lambda_2^x \lambda_2^y M_1^2 M_2^2 \end{aligned}$$

Here, f_+ is the FMR frequency of the acoustic mode whereas f_- is the FMR frequency of the optic mode.

To verify the theoretical prediction, we perform numerical simulations using the macrospin model. In the model, we solve the LLG equation with a small thermal fluctuation field (temperature = 1K) to keep the precession motion of magnetizations. Inset of Fig. 1(b) shows the time evolution of y -component of the magnetization, obtained for a SAF sample with $L = 120$ nm, $W = 60$ nm, $t_{F1} = t_{F2} = 2.5$ nm, $t_S = 1.0$ nm, $J_{ex} = -0.1$ erg/cm², $H_1^{k_0} = H_2^{k_0} = 10$ Oe, and $M_1 = M_2 = 1000$ emu/cm³. Fig. 1(b) shows the Fourier spectrum of the data in the inset of Fig. 1(b). The Fourier analysis reveals that there are two peak frequencies and thus two modes. A lower frequency peak corresponds to the acoustic mode whereas a higher one corresponds to the optic mode.

3. Results and Discussions

In Fig. 2, we show possible strategies of choosing the geometric and magnetic parameters in order to get a higher FMR frequency in a patterned SAF structure. Here, we have tested effects of i) the aspect ratio ($= L/W$) of the sample, ii) the thickness asymmetry ($= t_{F1}/t_{F2}$), and iii) the saturation magnetization ($M_S = M_1 = M_2$). The following parameters are used unless specified. The sum of the thicknesses of the free layer 1 (t_{F1}) and free layer 2 (t_{F2}) is fixed at 5 nm. The surface area ($=$ the product of the length (L) by the width (W)) is 7200 nm², and the thickness of Ru layer (t_S) is 1 nm. The magnetic parameters are; the crystalline anisotropy field $H_1^{k_0} = H_2^{k_0} = 10$ Oe, the damping constant $\alpha = 0.01$ in both FMs, and the RKKY exchange constant $J_{ex} = -0.1$ erg/cm². The external magnetic field is assumed to be zero.

Firstly, we show the dependence of FMR frequencies on the aspect ratio of the sample (Fig. 2(a)). The FMR frequencies of both modes increase with the aspect ratio. It is because the effective anisotropy field H_i^k including the crystalline and shape anisotropy fields increases with increasing the aspect ratio. In this case, the FMR frequency of the optic mode at $L/W = 3.125$ is about 14.1 GHz, which is much higher than the FMR frequency of the single layer with the same aspect ratio and the thickness of 2.5 nm. Secondly, we vary the thicknesses of each free layer whereas the sum of the thicknesses of both layers is fixed at 5 nm (Fig. 2(b)). The FMR frequencies increase as the thicknesses of two FMs become more asymmetric. It may be caused by the fact that as the thicknesses become more asymmetric, a thinner layer experiences a stronger coupling field consisting of the RKKY exchange field and the stray field from the other layer. Thirdly, we investigate the effect of the saturation magnetization M_S on the FMR frequency (Fig. 2(c)). The M_S is the same for both layers, and varied from 600 to 1500 emu/cm³. The FMR frequencies of both modes linearly increase with M_S . Note that H^k , H^d , and the dipolar coupling field are linearly proportional to M_S whereas λ^{RKKY} is inversely proportional to M_S^2 . The linear dependence of the FMR frequency on M_S indicates that the H^k , H^d , and dipolar coupling field are more dominant than the exchange coupling field in determining the FMR frequency when the pattern size is small.

REFERENCES

- [1] L. Savtchenko, B. N. Engel, N. D. Rizzo, M. F. Deherrera, and J. A. Janesky, U.S. Patent No. 6,545,906 (2003).
- [2] J. Hayakawa, S. Ikeda, Y. M. Lee, R. Sasaki, T. Meguro, F. Matsukura, H. Takahashi, and H. Ohno, *Jpn. J. Appl. Phys., Part 2* 45, L1057 (2006).
- [3] S. Ikeda, J. Hayakawa, Y. M. Lee, F. Matsukura, Y. Ohno, T. Hanyu, and H. Ohno, *IEEE Trans. Electron Devices* 54, 991 (2007).
- [4] A. M. Deac, W. H. Rippard, and J. A. Katine, *Digest of International magnetic conference (INTERMAG)*, CB-03 (2008).
- [5] D. Guskova, D. Houssameddine, U. Ebels, M. Cyril, B. Dieny, and L. Buda-Prejbeanu, *Digest of International magnetic conference (INTERMAG)*, CB-04 (2008).
- [6] S. Cornelissen, M. Op de Beeck, L. Lagae, L. Bianchini, Joo-Von Kim, T. Devolder, P. Crozat, and C. Chappert, *cond-mat/0810.1110v2* (2008).
- [7] J. C. Slonczewski, *J. Magn. Magn. Mater.* 159, L1 (1996).
- [8] L. Berger, *Phys. Rev. B* 54, 9353 (1996).
- [9] S. I. Kiselev, J. C. Sankey, I. N. Krivorotov, N. C. Emley, R. J. Schoelkopf, R. A. Buhrman, and D. C. Ralph, *Nature (London)* 425, 380 (2003).
- [10] P. Grünberg, *J. Appl. Phys.* 51, 4338 (1980).
- [11] R. E. Camley, T. S. Rahman, and D. L. Mills, *Phys. Rev. B* 23, 1226 (1981).
- [12] S. M. Rezende, C. Chesman, M. A. Lucena, A. Azevedo, and F. M. De Aguiar, *J. Appl. Phys.* 84, 958 (1998).
- [13] M. E. Schabes and A. Aharoni, *IEEE Trans. MAG.* 23, 3882 (1987).
- [14] K. S. Kim, K. J. Lee, and S. H. Lim, *Appl. Phys. Lett.* 93, 112503 (2008).
- [15] K. S. Kim, K. J. Lee, and S. H. Lim, *Appl. Phys. Lett.* 93, 152507 (2008).

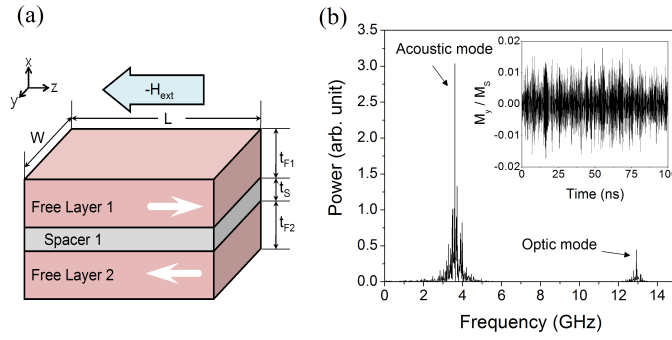


Fig. 1. (a) The illustration of SAF structure and the coordinate system. L and W are the length and the width of a patterned SAF film, respectively. t_{F1} , t_{F2} , and t_S are the thickness of free layer 1, free layer 2, and spacer (= Ru layer), respectively. (b) The power spectrum obtained from time evolution of the normalized y-component of magnetization shown in the inset of Fig. (b). A lower (higher) peak denotes the FMR frequency of acoustic (optic) mode. Data in the inset were obtained for a SAF sample with $L = 120$ nm, $W = 60$ nm, $t_{F1} = t_{F2} = 2.5$ nm, $t_S = 1.0$ nm, $J_{ex} = -0.1$ erg/cm², $H_1^{k_0} = H_2^{k_0} = 10$ Oe, and $M_1 = M_2 = 1000$ emu/cm³.

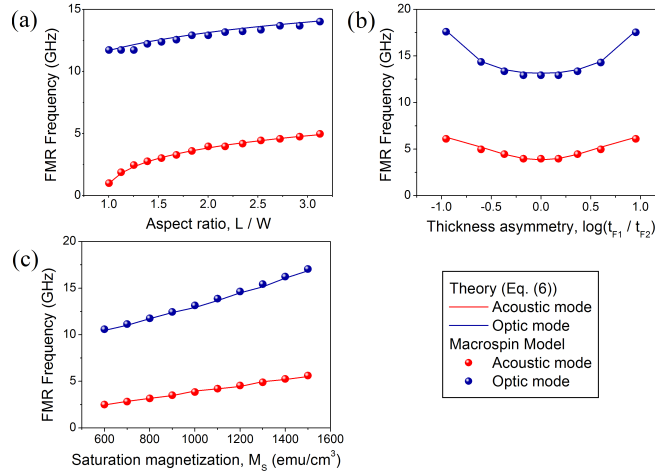


Fig. 2. (a) The FMR frequencies as a function of the aspect ratio (L/W). (b) The FMR frequencies as a function of the thickness ratio ($= t_{F1}/t_{F2}$) in the log-scale. (c) The FMR frequency as a function of the saturation magnetization of both FMs.